Solid-State Electronics 121 (2016) 41–46

Contents lists available at ScienceDirect

Solid-State Electronics

journal homepage: www.elsevier.com/locate/sse

Minority carrier injection and current–voltage characteristics of Schottky diodes at high injection level

Tigran T. Mnatsakanov [a], Michael E. Levinshtein [b,*], Alexey G. Tandoev [a], Sergey N. Yurkov [a], John W. Palmour [c]

[a] All-Russia Electrotechnical Institute, Krasnokazarmennaya 12, 111250 Moscow, Russia
[b] Ioffe Institute St. Petersburg, 26 Politekhnicheskaya, 194021, Russia
[c] Wolfspeed, A Cree Company, 3026 East Cornwallis Rd., Research Triangle Park, NC 27709, USA

ARTICLE INFO

Article history:
Received 3 February 2016
Received in revised form 28 March 2016
Accepted 14 April 2016
Available online 2 May 2016

The review of this paper was arranged by Prof. A. Zaslavsky

Keywords:
Schottky diodes
Silicon carbide
Forward bias
High current density
Minority carriers

ABSTRACT

Transport phenomena in Schottky diodes are analyzed at high injection levels of minority carriers. It is shown that the correct description of these phenomena requires that the mode of diffusion stimulated by the quasi-neutral drift (DSQD) should be considered. An analytical expression for current–voltage characteristics of a Schottky diode at high injection levels is derived. The expression predicts a seemingly paradoxical result: the higher the base doping level, the higher the voltage drop across a diode at the same current density. The analytical results are confirmed by computer simulations. The results may be important for analyses of SiC Junction Barrier Schottky (JBS) diodes at very high current densities (surge current mode).

1. Introduction

Schottky barrier diodes (SBDs) are a subject of considerable attention because of their fast switching speed and low forward voltage. They are widely used as a basic component for high speed electronic, optoelectronic and high-speed microelectronic applications, in personal computers, motor vehicles, and Power Factor Correction systems. The benefits of SBDs are due to the fact that Schottky diodes are majority carrier devices. In the conventional operation mode, no minority charge accumulates when a forward current flows.

However, it was noticed even in early studies of SBDs that although the minority-carrier injection from metal–semiconductor contacts is usually negligible at low current levels, the injection substantially increases on applying a sufficiently high forward bias [1]. Later, the phenomena associated with the accumulation of minority carriers in SBD bases have been extensively studied (see, e.g., Refs. [2–4]). It was noted that, in certain cases, a high injection level can be reached at high current densities. The most detailed study of the processes occurring in SBDs at high injection levels was carried out in the framework of the classical approach in Ref. [5].

Recently, the interest in the behavior of Schottky diodes in the presence of minority carriers re-appeared due to the emergence and rapid development of SiC SBDs. In the conventional SBDs, minority carriers may appear in the base if the Schottky barrier height exceeds half the band gap width E_g. Owing to the large value of E_g in silicon carbide (3.23 eV for the 4H polytype), it was believed that the problem of minority carriers is irrelevant to SiC SBDs. Nevertheless, the appearance of minority carriers in the base of Re/4H-SiC Schottky diodes was observed in the space-charge-limited current mode [6].

However, of particular interest is a study of the behavior of minority carriers in SiC Junction Barrier Schottky (JBS) diodes, suggested in [7] (see, e.g., Review [8]). A JBS diode is an integrated structure in which Schottky diodes are alternated with local p–n regions (Inset in Fig. 1). The p regions are closely spaced so that, under a reverse bias, the depletion regions of adjacent p–n junctions overlap each other. As a result, the leakage currents decrease to the values characteristic of reverse-biased p–n junctions. At the rated forward bias, the forward current flows only through the Schottky contact regions. When, however, the forward current density is high enough, the forward-biased p–n junctions inject

* Corresponding author. Tel.: +7 (812) 292 7988; fax: +7 (812) 297 1017.
E-mail address: melev@nimis.ioffe.ru (M.E. Levinshtein).

http://dx.doi.org/10.1016/j.sse.2016.04.004
0038-1101/

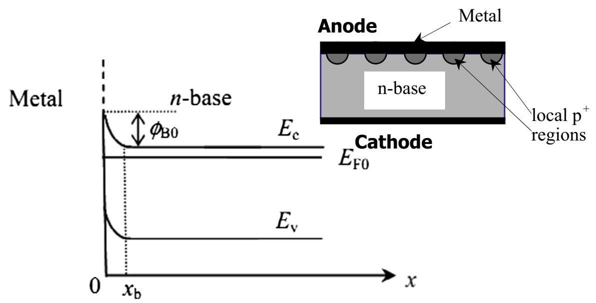

Fig. 1. Band diagram of the metal–semiconductor barrier at zero bias. Inset shows schematic of JBS structure.

minority carriers into the base of the structure and thereby make the forward voltage drop lower. It is noteworthy that surge currents in high-voltage high-power SiC structures may be as high as $\sim 10^4$ A/cm [9–11]. Meanwhile, the high-injection-level condition is satisfied in SiC JBS diodes even at substantially lower current densities.

It is important to note that the time of diffusion of minority carriers (holes in the JBS diode with an n-type base) between adjacent *p–n* junctions is considerably shorter than the characteristic duration of surge currents. Two types of surge pulses are distinguished by the international standards. These are the so-called "long" pulses (a half cycle of the 60 or 50 Hz sine wave or a 8–10 ms rectangular pulse) and "short" pulses", such as the 8/20 µs pulse, i.e., the pulse with 8 µs rise time and 20 µs fall time. However, rectangular current pulses with a characteristic pulse duration $t_0 \approx$ 20–50 µs are not infrequently used to characterize the ability of diodes to withstand a short-pulse current surge [10–12]. Taking the duration of the surge pulse to be t_p = 30 µs and the hole diffusion coefficient in SiC D_p = 3 cm^2/s, we find that the characteristic hole diffusion length during the pulse time is $L \sim (2b/(b+1)\cdot D_p \cdot t_p)^{1/2} \sim 230$ µm. Here $b = \mu_n/\mu_p$ where μ_n and μ_p are the low-field electron and hole mobilities, respectively. At the same time, the characteristic distance between the adjacent *p–n* junctions in JBS diodes is about 8–10 µm [8,13]. Thus, we can assume to a first approximation that the injection of minority carriers occurs uniformly over the entire area of the JBS diode.

When the forward current flows through a JBS diode, it can be represented as a parallel connection of an SBD and a *p–n* junction [14] (see Inset in Fig. 1). However, at the high current densities of a surge pulse, the current–voltage (I–U) characteristics of both the SBD and the *p–n* junction should be calculated by taking into account the effects described recently in Refs. [15,16] for *p–n* diodes. As shown in Ref. [15], *the mode of diffusion stimulated by the quasineutral drift (DSQD)* may be operative in addition to the well-known quasineutral modes of quasineutral diffusion and quasineutral drift. The DSQD mode fundamentally differs from the known diffusion and drift modes. In addition, as shown in Ref. [16], the field dependences of the electron and hole mobilities $\mu_n(F)$ and $\mu_p(F)$ should be taken into account even if the quasineutrality condition remains satisfied. The consequences of the occurrence of the DSQD mode and the $\mu(F)$ dependences were subjected to a consistent analysis in Refs. [15–17] only for *p–n* structures. However, preliminary numerical calculations show that these effects may be of fundamental importance for SBDs as well [15].

The purpose of this paper is to analyze the main specific features of *I–U* characteristics of SBDs in the presence of minority carriers at high current densities. The paper is organized as follows. In Section 2, the boundary condition determining the injection of minority carriers from the metal into the semiconductor is formulated. In Section 3, this boundary condition is used to solve the continuity equation for the base layer of the SBD. This solution makes it possible to determine and analyze the current–voltage characteristics of SBDs at high current densities. The analytical results obtained are verified and confirmed by a numerical simulation in Section 4.

2. The boundary condition determining the injection of minority carriers from the metal to the n-type semiconductor

The standard approach to formulating the boundary condition at the metal–semiconductor interface is based on balancing the current of majority carriers from the semiconductor to the metal (see, e.g., [18,19]). Consider for the sake of definiteness an SBD structure with an *n*-type base. The equilibrium band diagram of this structure is shown in Fig. 1.

We assume that the *Me-n* contact is situated at the point $x = 0$, and the point $x = x_b > 0$ corresponds to the boundary of the space charge region in the *n*-base layer. When a forward bias U is applied, the electron current density j_n flowing from the semiconductor to the metal is described in terms of the thermionic theory by the expression [18,20]:

$$j_n = j_s \exp\left(\frac{qU}{kT}\right), \tag{1}$$

where

$$j_s = A^* T^2 \exp\left(-\frac{q\phi_B}{kT}\right), \tag{2}$$

Here j_s is the saturation current density, A^* is the effective Richardson constant, k is the Boltzmann constant, $\phi_B = (E_C - E_F) + (\phi_{Me} - \phi_S)$, ϕ_{Me} is the work function of the metal, and ϕ_S is the work function of the semiconductor.

It is noteworthy that the barrier height ϕ_B depends on U (and, consequently, so does j_s). Indeed, at $U = 0$, ϕ_B contains the equilibrium Fermi level E_{F0}, and j_s is equal to j_{s0}:

$$j_{s0} = A^* T^2 \exp\left(-\frac{q\phi_{B0}}{kT}\right), \tag{3}$$

where $\phi_{B0} = E_C - E_{F0} + (\phi_{Me} - \phi_S)$. At a rather high forward bias U, minority carriers (holes) appear in the base due to the injection. In this case, the quasi-Fermi levels for electrons and holes, E_{Fn} and E_{Fp}, should be introduced. The saturation current density j_s is still described by expression (2), in which, however, the equilibrium value ϕ_{B0} should be changed to ϕ_{Bn}:

$$j_s = A^* T^2 \exp\left(-\frac{q\phi_{Bn}}{kT}\right), \tag{4}$$

where $\phi_{Bn} = E_C - E_{Fn} + (\phi_{Me} - \phi_S)$.

So, expression (1) can be rewritten as

$$j_n = j_{s0} \frac{\exp\left(-q(E_C - E_{Fn})/kT\right)}{\exp\left(-q(E_C - E_{F0})/kT\right)} \exp\left(\frac{qU}{kT}\right). \tag{5}$$

It can be easily seen that, in the quasi-equilibrium approximation, the following relations are valid at the point $x = x_b$:

$$\frac{\exp\left(-q(E_C - E_{Fn}(x_b))/kT\right)}{\exp\left(-q(E_C - E_{F0})/kT\right)} = \frac{n(x_b)}{n_0} \text{ and } \exp\left(\frac{qU}{kT}\right) = \frac{p(x_b)}{p_0}, \tag{6}$$

where n_0 and p_0 are the equilibrium electron and hole concentrations at $x = x_b$, respectively.

With (6) taken into account, expression (5) can be written as:

$$j_n(x_b) = j_{s0} \frac{n(x_b)p(x_b)}{n_i^2} = j_{s0} \frac{(p(x_b) + N_d)p(x_b)}{n_i^2}, \tag{7}$$

where $N_d = n_0$ is the doping level of the *n*-base and n_i is the intrinsic concentration. At low injection levels ($p \ll N_d$), a well known expression for the hole concentration at $x = x_b$ can be easily derived:

$$p(x_b) = \frac{n_i^2}{N_d}\frac{j_n}{j_{s0}}, \tag{8}$$

At high injection levels, however, $j_n = j_{s0}[p^2(x_b)/n_i^2]$, and the expression for then hole concentration at $x = x_b$ has the form:

$$p(x_b) = n_i\sqrt{\frac{j_n}{j_{s0}}}. \tag{9}$$

Relation (7) makes it possible to formulate the boundary condition for the continuity equation in the base layer. For this purpose, it is necessary to equate the electron current flowing from the semiconductor to the metal $j_n(x_b - 0)$ (expression (7)) to the electron current $j_n(x_b + 0)$ flowing to the point x_b from the base layer. At high injection levels, the general expression for the electron current $j_n(x_b + 0)$ has the form [16]

$$j_n(x_b + 0) = \frac{jb}{b+1} + \frac{jb}{(b+1)^2}\left(1 - \frac{j}{j_{crn}}\right)\frac{N_d}{p(x_b)} + q\frac{2b}{b+1}D_p\left.\frac{dp}{dx}\right|_{x_b}, \tag{10}$$

where $b = \mu_{n0}/\mu_{p0}$, $j_{crn} = q\left(\mu_{n0} + \mu_{p0}\right)N_d\left(F_{sn}^{-1} - F_{sp}^{-1}\right)^{-1}$; F_{sn} and F_{sp} are the fields at which the drift velocities of electrons and holes are saturated; and μ_{n0} and μ_{p0} are, respectively, the electron and hole mobilities at a low electric filed.

Equating expressions (7) and (10) for $j_n(x_b - 0)$ and $j_n(x_b + 0)$, we obtain the boundary condition governing the injection of minority carriers from the metal to the n-type semiconductor at high injection levels:

$$\left.\frac{dp}{dx}\right|_{x_b} = -\frac{j}{2qD_p} + \frac{j_{s0}}{qD_a}\frac{p^2(x_b)}{n_i^2} - \frac{j}{j_d}\left(1 - \frac{j}{j_{crn}}\right)\frac{N_d^2}{p(x_b)L}, \tag{11}$$

where $j_d = 2qD_p(b+1)N_d/L$, $L = \left(\frac{2b}{b+1}D_p\tau\right)^{1/2}$ is the ambipolar diffusion length, D_p is the hole diffusion coefficient, and τ is the minority carrier lifetime in the base.

This boundary condition differs from the well-known boundary condition for the p^+–n junction suggested in Ref. [21] in that an additional third term is introduced in right-hand side (11). The physical reason for this difference is the weak injection capacity (large j_{s0} values) of the metal–semiconductor junction. This leads to a decrease in the carrier concentration in the close vicinity of the junction and, as a consequence, to a rise in the field in this region. As a result, the contribution of the drift current component grows (see also (10)). The increase in this component makes it necessary to take into account the third term in the boundary condition (11). It is noteworthy that neglecting the third term in (11) in the case of the p–n junction is quite justified, as confirmed by numerous experimental data.

A boundary condition for analyzing Schottky diodes at high injection levels was suggested in Ref. [5]. This boundary condition also differs from (11) in having no third term in the right-hand side and virtually coincides with the corresponding boundary condition for the p–n junction (see Eq. (35) in [5]. As, however, is shown below, neglecting the third term in the right-side of (11) in the case of a Schottky diode may lead to qualitatively incorrect results.

3. Current–voltage characteristic of Me-n-n+ structure

Consider a *Me-n-n*$^+$ structure with an n-base of W width. As a rule, the condition $W/L < 1$ is valid for structures of this kind. Because the depletion layer thickness x_b is small at forward biases corresponding to high injection levels, we assume that the boundaries of the quasi-neutral region lie at $x = 0$ and $x = W$.

The *I–U* characteristic of such a structure is described by following standard expression:

$$U = \frac{kT}{q}\ln\left(\frac{p(0)p(W)}{n_i^2}\right) + \int_0^W F(x)dx; \tag{12}$$

where $p(0)$ and $p(W)$ are the hole concentrations at the boundaries of the base layer.

It can be seen in (12) that, to find the current–voltage characteristic of a structure, it is necessary to solve the continuity equation in the base and then, using the resulting $p(x)$ dependence, to calculate the terms in (12).

In the general case, the continuity equation at high injection levels is given by [16]:

$$\frac{d^2p}{dx^2} = \frac{j}{j_d}\left(1 - \frac{j}{j_{crn}}\right)\frac{N_d^2}{p^2}\frac{1}{L}\frac{dp}{dx} + \frac{p}{L^2}; \tag{13}$$

In this paper, we restrict our consideration to the case $j < j_{crn}$.

The boundary conditions for Eq. (13) have the form:

$$\left.\frac{dp}{dx}\right|_{x=0} = -\frac{j}{2qD_p} + \frac{j_{s0}}{qD_a}\frac{p^2(0)}{n_i^2} - \frac{j}{j_d}\left(1 - \frac{j}{j_{crn}}\right)\frac{N_d^2}{p(0)L}; \tag{14}$$

and

$$\left.\frac{dp}{dx}\right|_{x=W} = \frac{j}{2qD_n} - \frac{j_{sp}}{qD_a}\frac{p^2(W)}{n_i^2} \tag{15}$$

where j_{sp} is the saturation current of the n^+-n junction.

The nonlinearity of Eq. (13) makes it difficult to find its analytical solution. Therefore, we use the method of regional approximations [22]. It is necessary to take into account that j_{s0} in *Me-n-n*$^+$ structures exceeds the saturation current j_{sp} of the n^+-n junction by several (4–5) orders of magnitude. As a result, the hole concentration $p(0)$ is almost two orders of magnitude lower than $p(W)$. Then, with the $W/L < 1$ ratio taken into account, the hole concentration $p(x)$ increases monotonically from $p(0)$ to $p(W)$.

In accordance with the regional approximation method, we split the base region into two parts. In the region $0 \le x \le x_1$, adjacent to the *Me-n* contact, the hole concentration is relatively low. Therefore, the term in the right-hand side of the continuity Eq. (13), which describes the quasi-neutral drift, substantially exceeds the term describing the recombination loss of charge carriers.

As shown in [15,16], the continuity equation in this region has the form:

$$\frac{d^2p}{dx^2} - \frac{j}{j_d}\left(1 - \frac{j}{j_{crn}}\right)\frac{N_d^2}{p^2}\frac{1}{L}\frac{dp}{dx} = 0; \tag{16}$$

This form of the continuity equation corresponds to the *diffusion stimulated by quasi-neutral drift (DSQD)mode* [15,16].

In the region $x_1 \le x \le W$, adjacent to the *n-n*$^+$ junction, the hole concentration is high. Therefore, the continuity Eq. (13) in this region has the form corresponding to the diffusion mode:

$$\frac{d^2p}{dx^2} = \frac{p}{L^2}; \tag{17}$$

The coordinate of the point x_1 dividing the DSQD and diffusion regions is determined from the obvious condition:

$$\frac{j}{j_d}\left(1 - \frac{j}{j_{crn}}\right)\frac{N_d^2}{p(x_1)^2}\frac{1}{L}\left.\frac{dp}{dx}\right|_{x_1} = \frac{p(x_1)}{L^2}; \tag{18}$$

At this point, the solutions of Eqs. (16) and (17) and also their derivatives should be joined.

In the DSQD region ($0 \le x \le x_1$), the solution of Eq. (16) has the form:

$$\frac{p^*}{CL}\left[\frac{p(x)-p(0)}{p^*}+\frac{p^*}{CL}\ln\left(\frac{\frac{p(x)}{p^*}-\frac{p^*}{CL}}{\frac{p(0)}{p^*}-\frac{p^*}{CL}}\right)\right]=\frac{x}{L}; \tag{19}$$

where: $p^* = N_d\sqrt{\frac{j}{j_d}\left(1-\frac{j}{j_{crn}}\right)}$; $p(0) = n_i\sqrt{\frac{b}{b+1}\frac{j}{j_{s0}}\left(1+\frac{b+1}{b}\frac{qD_a p(W)}{jW}\right)}$; and $C = \frac{p(x_1)}{L}\left(\frac{p(x_1)}{p^*}\right)^2\left[1+\left(\frac{p^*}{p(x_1)}\right)^4\right]$;

In the diffusion region ($x_1 \le x \le W$), the solution of Eq. (17) has the form:

$$p(x) = Ae^{\frac{x}{L}} + Be^{-\frac{x}{L}}. \tag{20}$$

Taking into account the condition $W/L < 1$, we can represent (20) as

$$p(x) \approx a_1 x + a_2; \tag{21}$$

where $a_1 = \frac{p(W)-p(x_1)}{W-x_1}$; $a_2 = -\frac{p(W)x_1-p(x_1)W}{W-x_1}$; $p(W) = n_i\frac{\frac{2}{b+1}\frac{j}{j_i}}{1+\sqrt{1+\frac{4}{b+1}\frac{jj_{sp}}{j_i^2}}}$; $j_i = \frac{qDn_i}{W}$; and $p(x_1)$ is the root of Eq. (18), which, after some simple transformations, can be written as

$$\left(\frac{p(x_1)}{p^*}\right)^3+\frac{L}{W}\frac{p(x_1)}{p^*}-\frac{L}{W}\frac{p(W)}{p^*}=0; \tag{22}$$

The solution of Eq. (22) can be written by using the known Kardano formula [23]. With consideration for the condition $(p^*/p(W)) \ll 1$, this solution can be represented as

$$\frac{p(x_1)}{p^*}=\left(\frac{p(W)}{p^*}\frac{L}{W}\right)^{1/3}. \tag{23}$$

The solutions obtained allow us to find the terms in Eq. (12).

The voltage drop across the DSQD region ($0 \le x \le x_1$) is given by

$$U_{DSQD}=\frac{2b}{(b+1)^2}\frac{kT}{q}\frac{jW}{qDp(W)}\ln\frac{p(x_1)}{p(0)-p^*\frac{p^*}{p(W)}\frac{W}{L}} \tag{24}$$

The voltage drop across the diffusion region ($x_1 \leqslant x \leqslant W$) can be written as

$$U_{dif}=\frac{2b}{(b+1)^2}\frac{kT}{q}\frac{jW}{qDp(W)}\ln\frac{p(W)}{p(x_1)}; \tag{25}$$

The total voltage drop across the base region, U_W is the sum of the voltage drops across the DSQD and diffusion regions:

$$U_W=\frac{2b}{(b+1)^2}\frac{kT}{q}\frac{jW}{qDp(W)}\ln\frac{p(W)}{p(0)-p^*\frac{p^*}{p(W)}\frac{W}{L}}; \tag{26}$$

According to (12) and (26), the voltage drop across the Schottky diode is given by

$$U=\frac{kT}{q}\ln\left(\frac{p(0)p(W)}{n_i^2}\right)+\frac{2b}{(b+1)^2}\frac{kT}{q}\frac{jW}{qDp(W)} \times \ln\frac{p(W)}{p(0)-p^*\frac{p^*}{p(W)}\frac{W}{L}}; \tag{27}$$

It follows from (27) that the voltage drop across Schottky diode remains dependent on the base doping level *even when the injection level is high across the whole thickness of the base layer.*

The physical reason for this behavior was already mentioned in Section 2. It is related to the need to raise the electric field in the region in which the concentration of injected carriers is insufficient for providing a predetermined current transport within the standard approach used to describe the transport of free carriers (DSQD mode). Formally, the reason for the $U(N_d)$ dependence is the following. According to expression (27), the only factor dependent on N_d is p^* (see (19)). The rise in p^* with increasing N_d results in that the voltage drop U_w across the base layer becomes higher as N_d grows.

This important conclusion fundamentally contradicts with the results formulated for the high-level injection mode in Schottky diodes in Refs. [5,18]. According to the results obtained in these papers, the voltage drop across the Schottky diode is independent of the base doping level at high injection level.

Fig. 2 compares the current–voltage characteristics of identical Schottky diodes calculated by the "classical" approach with consideration for the presence of the DSQD region. Fig. 2a shows the current–voltage characteristics calculated by using formula (27). Fig. 2b presents the current–voltage characteristics calculated with the "classical" boundary condition [5,18], in which the third term in the right-hand side of (11) is dropped.

In both cases, calculations were made for a Si Schottky diode with a base layer thickness $W = 100$ μm and $W/L = 0.5$. The saturation current densities j_{so} and j_{sp} were 2×10^{-8} and 2×10^{-12} A/cm^2, respectively. The height of the Schottky barrier at zero bias, ϕ_{B0}, was taken to be 0.85 eV. As mentioned above, formula (27) is valid for current densities $j < j_{crn.} = q\left(\mu_{n0}+\mu_{p0}\right)N_d\left(F_{sn}^{-1}-F_{sp}^{-1}\right)^{-1}$. Taking $F_{sn} \approx v_s/\mu_{n0} \approx 7 \times 10^3$ V/cm and $F_{sp} \approx v_s/\mu_{p0} \approx 2.2 \times 10^4$ V/cm in the simplest "two-piece approximation", we can easily verify that the condition $j < j_{crn}$ is valid for all the dependences in Fig. 2. (Here $v_s \approx 10^7$ cm/s is the saturated drift velocity of carriers.)

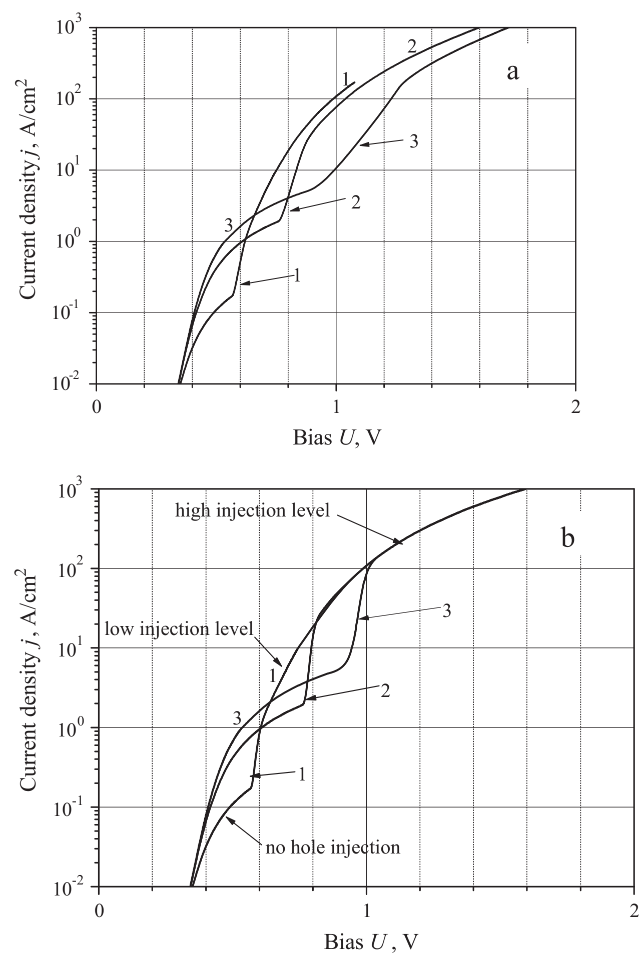

Fig. 2. Current–voltage characteristics calculated for identical Schottky diodes with different boundary conditions. The curves in figure (a) are calculated by (27). The dependences in figure (b) are calculated with the "classical" boundary condition in which the third term in the right-hand side of (11) is dropped. Doping level of the base layer, N_d (cm^{-3}): (1) 5×10^{13}, (2) 3×10^{14}, (3) 6×10^{14}.

It is seen that the current–voltage characteristics in Fig. 2a and b fully coincide for the biases at which there is no injection of minority carriers. They also nearly coincide at relatively small biases in the presence of injected holes at low injection levels. As expected, the voltage drop across the diode at low injection levels is the lower, the higher the base doping level N_d (for the same current density). However, at high current densities at which the high-injection-level condition is satisfied, calculations at different boundary conditions predict fundamentally different results. The calculation for the "classical" boundary conditions [5,18] (Fig. 2b) predicts that the voltage drop at high injection levels is independent of N_d. This result corresponds to the statement repeatedly made in the literature: at high injection levels at which the free-carrier concentration $p \approx n \gg N_d$, the voltage drop should be independent of the doping level.

By contrast, taking into account the DSQD mode in the boundary condition (third term in (11)) predicts a seemingly paradoxical result: the higher the doping level, the higher (at the same current density) the voltage drop across the Schottky diode.

4. Numerical simulations

To verify the analytical results obtained in Sections 2 and 3, we calculated numerically the current–voltage characteristics of Schottky diodes. The calculations were made with the "INVESTIGATION" software. A detailed description of the software was given in [24,25]. This software package solves numerically a fundamental system of equations, which comprises two continuity equations (for electrons and holes) and a Poisson equation. The continuity equations are written in a form that takes into account all the main non-linear phenomena in bipolar devices: electron-hole scattering, semiconductor bandgap narrowing, and Auger recombination. The program also takes into consideration the decrease in the carrier lifetime and mobilities in the highly doped p^+ and n^+ layers. The INVESTIGATION software has already been used to analyze steady-state and transient processes in Si and SiC diodes and thyristors (see, e.g., [26,27]).

The calculations were performed for a silicon Schottky diode with the same parameters that were used in the analytical calculations (Fig. 2). The lifetime τ at high injection levels was 22 μs, which corresponds to $W/L = 0.5$. The doping level of the 20-μm-thick emitter n^+-region was 1×10^{20} cm^{-3}. The height of the Schottky barrier at zero bias ϕ_{B0} was 0.85 eV.

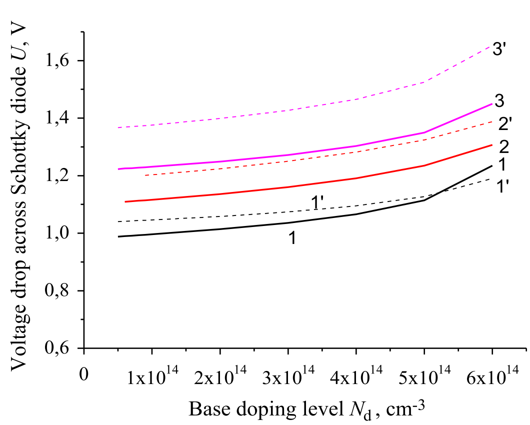

Fig. 3. Dependences of the voltage drop across the Schottky diode on the base doping level N_d at three current densities j(A/cm^2): (1,1′) 100, (2,2′) 200, (3,3′) 300. The solid lines represent the dependences calculated analytically by (27). The dashed lines show the results of numerical simulations. The high-injection-level condition is satisfied for all the dependences.

Fig. 3 demonstrates the results of calculations.

It is seen that the rise in the voltage drop across the diode with increasing N_d, predicted by the analytical theory, is observed for all the current densities. At a current density $j = 100$ A/cm^2, the analytical and numerically calculated results agree reasonably well. With increasing current density, the quantitative difference between the analytical and numerical results grows. The numerical calculations show that this is due to the inaccuracy of the regional approximation method. However, as can be seen from Fig. 3, the effect predicted by the analytical theory is observed in all cases.

5. Conclusion

It is shown that the mode of diffusion stimulated by the quasineutral drift (DSQD) should be taken into account to correctly describe the transport phenomena in Schottky diodes at high minority carrier injection levels. The boundary condition determining the minority carrier injection from a metal to a semiconductor is formulated. This boundary condition makes it possible to take into account the occurrence of the DSQD mode. With this boundary condition, the analytical expression for the current–voltage characteristic of the Schottky diode at a high injection level was derived by using the regional approximation technique. The resulting expression predicts a seemingly paradoxical result: the higher the base doping level, the higher the voltage drop across the diode at the same current. This result strongly contradicts the "classical" result for high injection levels. In accordance with the "classical" consideration, the voltage drop should be independent of the doping level at high injection levels at which the free-carrier concentration $p \approx n >> N_d$. The analytical results obtained in the study are confirmed by an adequate computer simulation. These results are significant for analyses of SiC Junction Barrier Schottky (JBS) diodes in surge current modes.

Acknowledgment

At the Ioffe Institute and All-Russian Electrotechnical Institute this work was partly supported by Wolfspeed, A Cree company.

References

[1] Scharfetter DL. Solid State Electron 1965;8:299–311.
[2] Yu A, Snow E. Solid State Electron 1969;12:155–60.
[3] Green A, Shewchun J. Solid State Electron 1973;16:1141–50.
[4] Elfsten B, Tove PA. Solid State Electron 1985;28:721–7.
[5] Ng WT, Liang S, Salama CAT. Solid State Electron 1990;33:39–46.
[6] Sarpatwari K, Mohney SE, Ashok S, Awadelkarim OO. Phys Stat Solidi (a) 2010;207:1509–13.
[7] Held DR, Kaminski N, Niemann E. 1997 Proceedings of the 7-th International Conference on Silicon Carbide and Related Materials, Stokholm, Sweden, Materials Science Forum 264–268, p. 1057–60 .
[8] Zhao JH, Sheng K, Lebron-Velilla RC. Silicon Carbide Schottky barrier diodes. In: Shur M, Rumyantsev S, Levinshtein M, editors. SiC Materials and Devices – vol. 1. Singapore – New Jersey – London – Hong Kong: World Scientific; 2006.
[9] Levinshtein ME, Ivanov PA, Mnatsakanov TT, Palmour JW, Das MK, Hull BA. Solid State Electron 2008;52:1802–5.
[10] Hillkirk LM. Solid State Electron 2004;48:2181–9.
[11] Levinshtein ME, Mnatsakanov TT, Ivanov PA, Palmour JW, Das MK, Hull BA. Semicond Sci Techn 2008;23:085011.
[12] Maas BL, Clements ND, Rinaldi V. IEEE Trans Mag 1993;29:1017–24.
[13] Ivanov PA, Grekhov IV, Potapov AS, Kon'kov OI, Ilyinskaya ND, Samsonova TP, et al. Semiconductors 2012;46:397–400.
[14] Buttay C, Raynaud C, Morel H, Civrac G, Locatelli M-L, Morel F. IEEE Trans Electron Dev 2012;59:761–9.
[15] Mnatsakanov TT, Levinshtein ME, Tandoev AG, Yurkov SN. J Appl Phys 2009;105:044506.
[16] Mnatsakanov TT, Tandoev AG, Levinshtein ME, Yurkov SN. Semicond Sci Technol 2009;24:075006.
[17] Mnatsakanov TT, Tandoev AG, Levinshtein ME, Yurkov SN. Solid State Electron 2011;56:60–7.
[18] Sce SM. Physics of semiconductor devices. New York: John Wiley & Sons; 1981.
[19] Shur MS. GaAs devices and circuits. New York: Plenum Press; 1987.
[20] Crowell CR, Sze SM. Solid State Electron 1966;9:1035–48.

[21] Herlet A. Solid State Electron 1968;8:717–42.
[22] Lampert M, Mark P. Current injection in solids. New York and London): Academic Press; 1970.
[23] Korn GA, Korn TM. Mathematical handbook for scientists and engineers. New-York Toronto-London: McGraw-Hill Book Company Inc.; 1961.
[24] Mnatsakanov TT, Rostovtsev IL, Philatov NI. Solid-State Electron 1987;30:579–85.
[25] Mnatsakanov TT. Phys Stat Solidi (b) 1987;143:225–34.
[26] Mnatsakanov TT, Levinshtein ME, Pomortseva LI, Palmour JW. Semicond Sci Technol 2009;24:125011.
[27] Mnatsakanov TT, Levinshtein ME, Tandoev AG, Yurkov SN. J Appl Phys 2013;119:064503.